RSC Advances

ROYAL SOCIETY OF CHEMISTRY

www.rsc.org/advances

Cite this: DOI: 10.1039/c0xx00000x

www.rsc.org/xxxxxx

ARTICLE TYPE

Novel carbon dots/BiOBr nanocomposites with enhanced UV and visible light driven photocatalytic activity

Qingqing Du, Wenpeng Wang, Yongzhong Wu*, Gang Zhao, Fukun Ma, XiaopengHao*

Received (in XXX, XXX) Xth XXXXXXXXX 20XX, Accepted Xth XXXXXXXXX 20XX

DOI: 10.1039/b000000x

Novel UV and visible light photocatalytic carbon dots/BiOBr nanocomposites were prepared for the first time. The structures, morphologies, optical, photoelectrochemical and photocatalytic properties were investigated. The results indicated that the carbon dots (CDs) were combined well with the BiOBr. Proper amount of introduced CDs can significantly enhance the photocatalytic activities under both UV and visible light irradiation. The enhanced activities were mainly attributed to the enhanced light absorption and the interfacial transfer of photogenerated electrons. The corresponding photocatalytic mechanism was proposed based on the results.

1. Introduction

The exploration and design of new photocatalysts with good stability and high catalytic efficiency in sunlight is a core issue in photocatalysis field all the time, and is also significant in solving current environment and energy problems. Over the past decades, semiconductor-based photocatalysts have attracted considerable research attentions for degradation of organic compounds due to its potential to purify wastewater that is discharged from industry and households.[1,2]Among the known materials, bismuth oxybromide (BiOBr), an important V–VI–VII ternary compound, possessing internal electric fields in sandwich like crystals, has received great research interest due to its eco-friendly, stability, suitable band gaps and relatively superior photocatalytic abilities.[3]Despite these advantages, photocatalytic activity of the pure BiOBr has been limited by the high recombination of the photogenerated electron–hole pairs, it is still necessary to further enhance its photocatalytic activity for practical applications. In order to improve the photocatalytic performance of BiOBr, $ZnFe_2O_4$, [4]AgBr, [5] g-C_3N_4[6]and graphene[7], etc. have been coupled with BiOBr to prepare nanocomposites. AgBr/BiOBr composite exhibited enhanced photocatalytic activity due to the band structure and synergistic effect within the p–n junctions.[5]However, AgBr usually suffer from significant deactivation and lost their photoactivity.[8,9] Furthermore, superior photocatalytic performance has also been observed over graphene/BiOBr, which is attributed to the great adsorption of dyes, the extended photoresponse range and the high migration efficiency of photoinduced electrons. On the other hand, graphene is easy to aggregate and difficult to disperse in common solvents, which will limit their wide applications.[10]The results indicate that coupling is an effective means to improve the photocatalytic activity and further development for modification of BiOBr is needed. Especially, quantum dots with stability, high aqueous solubility, uniform distribution, intimately contacted interface and excellent charge transfer ability are worth of expectation to modify BiOBr and further enhance the photocatalytic activity.[11]

Carbon dots (CDs), a novel class of oxygen-containing carbonaceous nanomaterials, have been attracting increasing attention. Compared with the conventional narrow band gap nanomaterials, it possess many good characteristics, such as high aqueous solubility, low toxicity, good biocompatibility, easy functionalization and photoinduced electron transfer property, which indicate that CDs can act as an efficient component in design of photocatalyst.[12, 13]Owing to the small size and rich functional groups of CDs, the composite structures could form sufficient contraction with uniform distribution. In addition, due to the excellent charge transport properties, it could further construct the bulk to surface channels for the electrons. What's more, conjugated materials are a category of materials with unique properties in electron or hole transport. Due to the conjugated π structure of CDs, it can exhibit the excellent electron transfer/reservoir properties.[14]Very recently, CDs have been introduced into semiconductors successfully and boost their photocatalytic performance. Lee et al. first proved the availability of TiO_2/CDs and SiO_2/CDs hybrids for efficient improves the photocatalytic performance.[15]Afterwards, CDs have been blended with Fe_2O_3, Ag_3PO4, Cu_2O, ZnO and hematite for the degradation of dyes and toxic gases.[16-20]

Considering such remarkable properties of CDs and BiOBr mentioned above, functionalizing CDs with BiOBr can combine both advantages of these two materials. The CDs/BiOBr nanocomposites are expected to be an ideal system with good stability and higher photocatalytic performance. To the best of our knowledge, the preparation and investigation of CDs/ hybrids toward organic pollutant degradation under UV and visible light have not been previously reported to date.

Herein, we report the fabrication of novel CDs/BiOBr nanocomposites photocatalysts for the first time. The structures, morphologies, optical, electrochemical and photocatalytic

properties were investigated. The photocatalytic activities of the CDs/BiOBr nanocomposites were evaluated sufficiently by the photocatalytic degradation of RhB. It was found that the CDs could enhance the light utilization and separation efficiency of photogenerated electrons and holes. Thus both the photocatalytic activities under the UV and visible light irradiation enhanced significantly. Accordingly, a reasonable mechanism of pollutant photodegradation in this system was proposed based on the measurements of the transient photocurrent response and free radicals trapping experiments.

2. Experimental section

2.1 Preparation

All chemicals were of analytical grade and used without further purification. BiOBr were prepared by solvothermalmethod.[21] In a typical procedure, 0.001 mol of $Bi(NO_3)_3 \cdot 5H_2O$ was dissolved into ethylene glycol (EG) solution containing stoichiometric amounts of ionic liquid1-butyl-3-methylimidazolium bromide ([BMIM] Br) and 0.25g polyvinyl-pyrrolidone (PVP K30), the mixture was stirred for 30 min, and then was transferred into 25mL Teflon-lined autoclave up to 80% of the total volume. The autoclave was then heated at 140℃ for 24 h and cooled down to room temperature. The final product was separated by centrifugation, washed with distilled water and absolute ethanol for three times, and dried under vacuum at 50℃ for 24 h.

CDs was synthesized according to the literature followed by freeze-drying.[22]A suitable amount of glucose was dissolved in deionized water (50 mL) to form a clear solution (1 mol/L). NaOH (50 mL, 1 mol/L) solution was added into the solution of glucose, and then the mixed solution was treated ultrasonically for 2 h. The raw samples (20 mL) obtained from glucose/NaOH were first adjusted to pH = 7 with HCl, then added 100 mL ethanol drop by drop into the solution under stirring. After that, the solution of CDs was treated by adding a suitable amount of $MgSO_4$ (10 ~12 wt. %), stirred for 20 min and stored for 24 h to remove the salts and water.

100mg BiOBr was dispersed in CDs solution and kept stirring for 12 h to prepare the CDs/BiOBr nanocomposites. CDs/BiOBr nanocomposites prepared by changing the amount of CDs solution of 1, 2, 4 and 8 mL were labeled as 1mL-CDs/BiOBr 2mL-CDs/BiOBr, 4mL-CDs/BiOBr and 8mL-CDs/BiOBr, respectively. The obtained samples were washed with water, and then dried in an oven at 60℃ overnight.

2.2 Characterization

Powder X-ray diffraction (XRD) patterns were recorded on a Bruker D8-Avance X-ray powder diffractometer with a Cu-Kα radiation tube over the range of $10^o \leq 2\theta \leq 80^o$ (λ=0.154056 nm, the accelerating voltage and the applied current were 40 kV and 35mA, respectively). Scanning electron microscopy (SEM) images and EDS elemental mapping were collected using a Hitachi S-4800 microscope equipped with an energy-dispersive X-ray analyzer (EDS, Horiba EMAX Energy EX-350). The transmission electron microscope (TEM) analyses were carried out with a JEM-100CX field emission electron microscope. UV-vis diffuse reflectance spectra (DRS) were obtained with a Shimadzu UV2550 recording spectrophotometer equipped with an integrating sphere from 200 to 800 nm. $BaSO_4$ was used as a reference. X-ray photoelectron spectroscopy (XPS, Thermo ESCALAB 250) was performed using monochromated Al Ka radiation (1486.8eV). The photoluminescence spectra of the photocatalysts were detected using an Edinburgh FLS920 spectrometer.

2.3 Photocatalytic activity measurements

The photocatalytic activity of the samples was evaluated by monitoring the degradation of RhB under light from 500 W mercury or Xe lamp equipped with cutoff filters (λ ≥420 nm) to provide UV and visible light, respectively. Typically, 20mg photocatalysts were dispersed in 40mL 20mg/L RhB solution. Prior to irradiation, the suspensions were magnetically stirred in the dark for 1h to reach adsorption equilibrium. At certain time intervals, 3.5mL suspensions were sampled and centrifuged (10000rpm, 3min) to remove the catalyst. The degraded solutions were examined by measuring the absorbance at 553nm on a UV-vis spectrometer (Shimadzu UV-2500). To investigate the active species generated in the photodegradation process, the experiments of free radicals (•OH and h^+) capture were carried out by tert-butanol (TBA) and EDTA-2Na, respectively.

2.4 Photoelectrochemical activity measurements

Photoelectrochemical test systems were composed of a CHI660D workstation (Shanghai Chenhua, China) with a three-electrode configuration using the prepared samples as the working electrodes, a Pt plate as the counter electrode, Ag/AgCl as the reference electrode and a 50 W Xe lamp served as the light source. 0.5M Na_2SO_4 aqueous solution was used as the electrolyte. Working electrodes were prepared as follows: 20 mg as-prepared nanocomposites were dispersed in absolute ethanol, and then the suspension was directly deposited onto an indium-tin oxide (ITO) glass plate and then dried at 80 ℃in a vacuum oven. Electrochemical impedance measurements (EIS) were performed over the frequency range from 0.1 to 100 kHz.

3. Results and discussion

3.1 Structure, morphology and chemical composition characterization

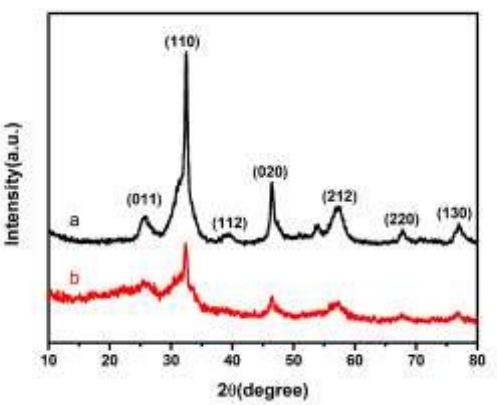

Fig. 1 XRD patterns of (a) BiOBr and (b) 2mL-CDs/BiOBr nanocomposites.

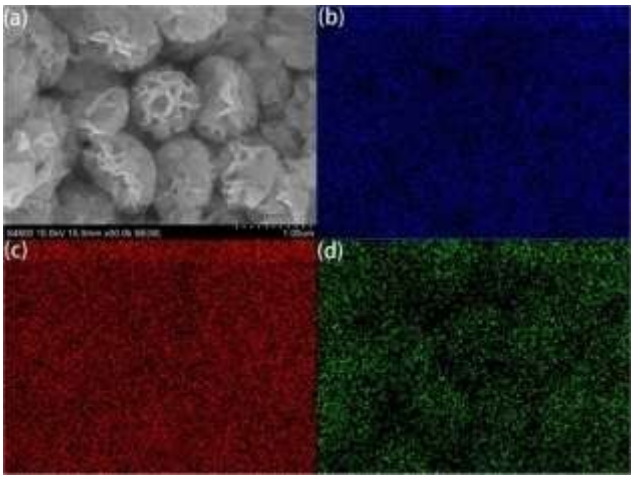

Fig. 2 SEM images (a) and EDS elemental mapping of Br (b), Bi (c) and C (d) of 2mL-CDs/BiOBr nanocomposites.

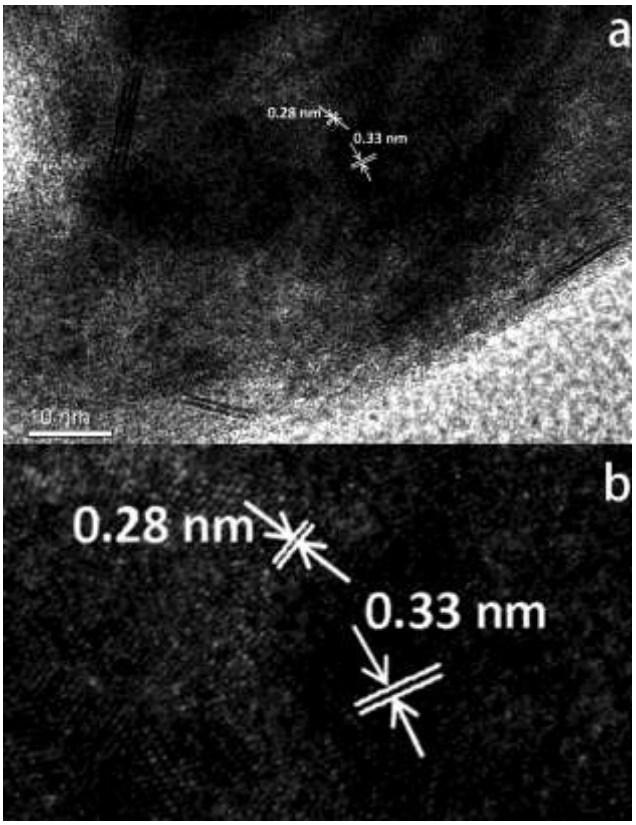

Fig. 3 TEM micrograph of the 2mL-CDs/BiOBr nanocomposites (a) and partial enlarged HRTEM view (b).

Fig. 1 shows the XRD patterns of the as-prepared BiOBr and 2mL-CDs/BiOBr samples. For the spectra of pure BiOBr (black line), characteristic diffraction peaks of (011), (110), (112), (020), (212), (220) and (130) were detected, which can be ascribed to thetetragonal BiOBr (JCPDS 73-2061). The diffraction peaks for the 2mL-CDs/BiOBr nanocomposites (red line) were similar to the BiOBr and no characteristic diffraction peak for CDs was observed, which may because of its low quantity, small size and high dispersion of CDs, in agreement with previous reports.[23]There was also no evident shift of the characteristic diffraction peaks in the spectra for the CDs/BiOBr composites, suggested that the deposited CDs were not incorporated into the BiOBr lattice.[3]

The morphology and microstructure of the as-obtained 2mL-CDs/BiOBr nanocomposites were studied by SEM and TEM. Fig.2a presented the SEM micrographs of the CDs/BiOBr nanocomposites sample. The products are flower-like microspheres, which consist of numerous two dimensional nanosheets. Besides, the EDS pattern (Fig. S2) shows that the 2mL-CDs/BiOBr sample contain C, O, Br and Bi elements. The associated EDS elemental maps (Fig. 2b-d) were obtained to evaluate the chemical uniformity within the samples, which clearly confirms that CDs are evenly distributed on the surface of BiOBr spheres. TEM and HRTEM analysis was applied to further explore the structure of the 2mL-CDs/BiOBr nanocomposites (Fig. 3 a and b), revealing the interplanar spacing of 0.28 nm and 0.33 nm, which corresponds to the (110) crystal planes of BiOBr and the (002) crystal planes of graphite, respectively. It can be seen that the tiny CDs are closely attached to the surface of BiOBr nanosheets. The combination of two parts gives a rise in synergistic properties arising from the intimately contacted interface interaction, which can benefit better charge separation and efficient electron transfer, corroborating the enhanced photocatalytic activity.

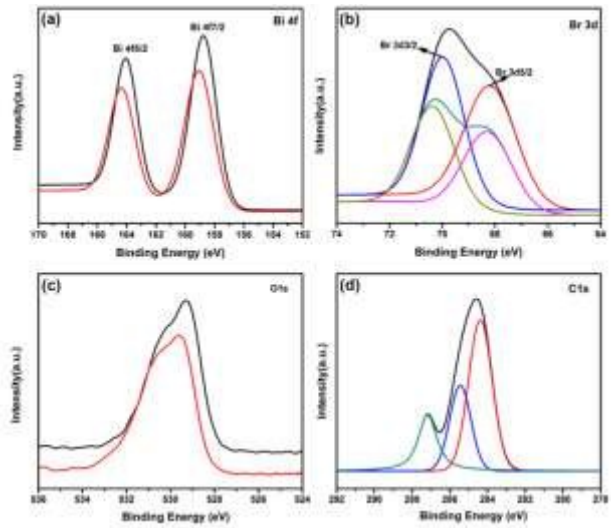

Fig. 4 XPS spectra of the pure BiOBr (black line) and 2mL-CDs/BiOBr (red line), (a)Bi 4f, (b)Br 3d, (c) O 1s and (d) C 1s.

XPS was used to study the components and surface properties of the CDs/ BiOBr nanocomposites. From the Bi4f XPS spectra shown in Fig. 4a, two strong peaks centered at 164.1eV and 158.8eV were observed, belonging to Bi 4f5/2 and Bi 4f7/2, respectively, which are corresponding to Bi^{3+}in crystal structure.[24]The Bi 4f peaks in the CDs/BiOBr nanocomposites display a slight blue-shift compared to bare BiOBr sample, which probably arises from the coupling of BiOBr with CDs. The XPS spectrum of Br 3d (as seen in Fig. 4b) showed two individual Br 3d 3/2andBr 3d5/2 peaks, with binding energy of 69.9eV and 68.2eV, respectively, indicating that the Br elements were mainly in the form of Br^-.[24]The O 1s peaks at529.5eV (Fig. 4c) can be assigned to the oxygen in BiOBr crystals. Fig. 4d shows the high-resolution XPS spectra of C 1s. The main peakat 284.4eV is ascribed to the C-C bond with sp^2orbital.The deconvoluted XPS

peaks ofthe C1s centered at the binding energyof 285.4eV and 287.1eV are assigned to the sp^3 hybridized carbons and C=O, respectively, suggesting the presence of the CDs in the CDs/BiOBr nanocomposites, whichis well consistent with the HRTEM result.[25]

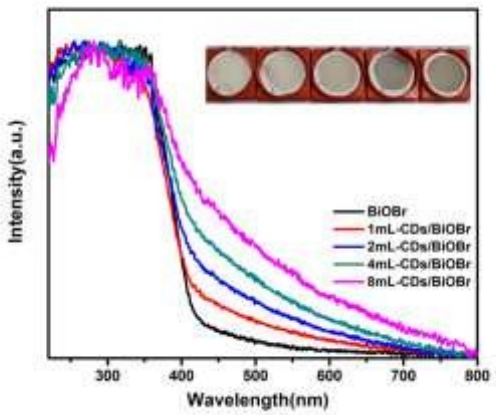

Fig. 5 UV-vis-DRS and photos of the as-prepared powder samples.

Photoabsorption is one of the key factors affecting the photocatalytic performance of photocatalysts. The optical properties of pure BiOBr and CDs/BiOBr with different CDs contents were probed with UV-vis diffuse reflectance spectroscopy (Fig. 5). On the macro level, the introduction of CDs deepened the color of the composites from light yellow to gray-brown, which indicated the absorption of visible light was enhanced. Compared to the pure BiOBr, all of the CDs/BiOBr samples prepared exhibited enhanced absorption in the visible light region due to thepresence of CDs on the BiOBr surface. Furthermore, the absorption intensity of the CDs/BiOBr samples increased with increasing CDs content. It suggests that CDs play important roles in utilizing sunlight and increasing electric surface charge of the oxide within the composite, which can possibly cause modifications of the fundamental process of electron-hole pair formation during irradiation.[14]

3.2. Photocatalytic properties

The photocatalytic activityof the as-prepared samples was evaluated by degradation the organic contaminant RhB in aqueous solution under UV or visible light irradiation. Fig. 6a and c display the photocatalytic activity of the CDs/BiOBr nanocomposites with different CDs contents as well as pure BiOBr under UV and visble light, respectively. The photolysis tests show that RhB was hardly degradated in the absence of photocatalysts. It was observed that all of the CDs/BiOBr samples exhibited higher photocatalytic performance than pure BiOBr. Moreover, the degradation efficiency increased gradually with the increased CDs content at the beginning from 1 to 2mL. The 2mL-CDs/BiOBr sample exhibited the highest degradation activity and excess amount of CDs leaded to a decrease of degradation efficiency. Because overloading of CDs can result in a light harvesting competition and shield the light from reaching the surface of BiOBr.[26]What's more, the added CDs tend to accumulate on surface and porosity, which may impede the diffusion and convection of solution; it is probably another reason for the decreasing photocatalytic performance.[27]The kinetic constant of pure BiOBr and 2mL-CDs/BiOBr nanocomposites was determined from the pseudo-first-order reaction rate equation of $\ln(C/C_0) = KT$, where C_0 is the initial concentration of RhB, C is the concentration of RhB at interval time, K is the kinetic constant. As is shown in Fig. 6 b and d, the photocatalytic degradation rate was improved through the introduction of CDs under both UV and visible light irradiation.

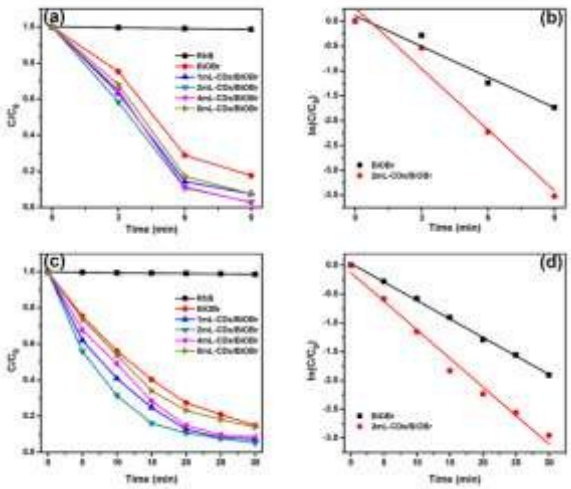

Fig. 6 Variation of normalized C/C_0 concentration of RhB with irradiation time and the reaction kinetics under UV (a, b) and visiblelight (c, d) irradiation.

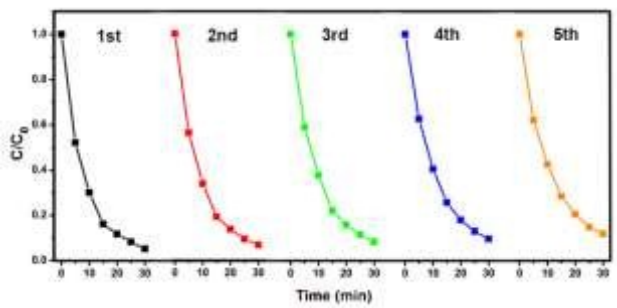

Fig. 7 Recycling tests of 2mL-CDs/BiOBr under visible light irradiation.

Stability and reusability is of vital importance for photocatalysts in practical applications. A five-cycle photodegradation sequence for 2mL-CDs/BiOBr was carried out in degradation of RhB (at the same initial concentration) under UV and visible light, respectively (shown in Fig.S3 and Fig. 7). During the repeated experiments, there was no significant loss of photocatalytic activity. Therefore, the as-prepared CDs/BiOBr nanocomposites can work as effective photocatalysts for organic compounds degradation with good stability in the absence of electron acceptors.

3.3. Mechanism of photocatalytic activity enhancement

All of the above experimental results demonstrated that the introducing CDs to BiOBr play key roles for the enhanced photocatalytic activity. Therefore, it is significant to investigate the role of CDs in the nanocomposites.

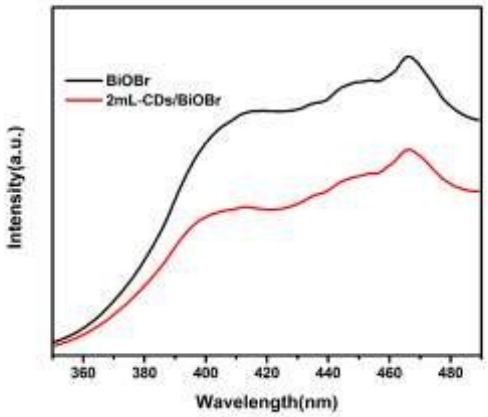

Fig. 8 PL spectra of the pure BiOBr and 2mL-CDs/BiOBr nanocomposites.

Photoluminescence (PL) spectra have been widely used to reveal the charge transfer, migration and recombination processes in photocatalysts. As is shown in Fig. 8, the pure BiOBr had a strong emission peak at around 460nm under excitation at 250nm, which was due to the recombination of the electron–hole pairs. After CDs were anchored on the BiOBr surface, the intensity of this emission peak decreased significantly. As is known, weaker intensity represents lower recombination probability of photoexcited charge carriers.[28]It was proved that the recombination of the photo-excited electrons and holes was greatly restrained by coupling CDs and BiOBr and thus improved the photocatalytic activities. Therefore, it can be speculated that the introduction of CDs to BiOBr matrix may contribute to improving the photocatalytic activity of BiOBr.

The electrochemical experiments were also conducted to further investigate the separation of photogenerated charge carriers. It is widely accepted that the photocurrent is mainly determined by the electron-hole pair separation efficiency within the photoelectrodes.[29]Thetransient photocurrent responses of pure BiOBr as well as 2mL-CDs/BiOBr were recorded for several on–off cycles of irradiation. As seen in Fig. 9 (a), the photocurrent increased sharply upon light irradiation and returned quickly to its dark-current state when the light was turned off. The photocurrents were steady and reproducible during several intermittent on–off irradiation cycles. The 2mL-CDs/BiOBr nanocomposites exhibited enhanced photocurrent response compared to the pure BiOBr, which further indicated that the recombination of the photogenerated charge carriers was greatly inhibited attributed to the coupling with CDs, which served as electron-acceptor/donor material due to the conjugated π structure and acted as the separation center of the photoexcited charge carriers.[30,31]Electrochemical impedance spectroscopy (EIS) measurements were used to investigate charge transfer and recombination processes at solid/electrolyte interfaces. It was observed in Fig. 9 (b) that the diameter of the arc radius on the EIS Nynquist plot of the 2mL-CDs/BiOBr nanocomposites electrode was smaller than that of the bare BiOBr electrode under UV-visible light irradiation, which indicated a more effective separation of photogenerated electron-hole pairs and faster interface charge transfer.[32,33]The results of photocurrents and EIS measurements were consistent with the PL analysis, which confirm that the introduction of CDs is an effective way to improve photocatalytic efficiency.

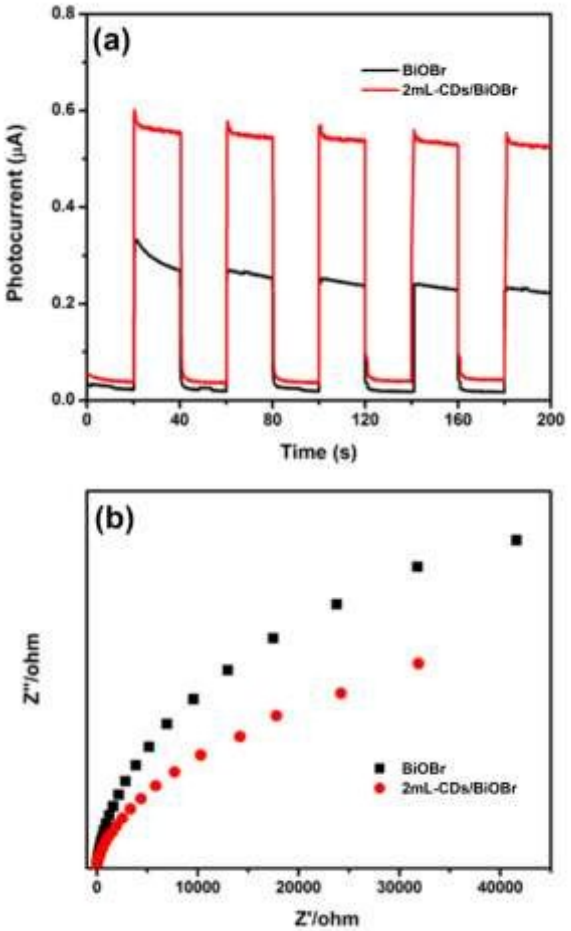

Fig. 9 (a) Transient photocurrent response and (b) Nyquist impedance plots of the pure BiOBr and 2mL-CDs/BiOBr nanocomposites.

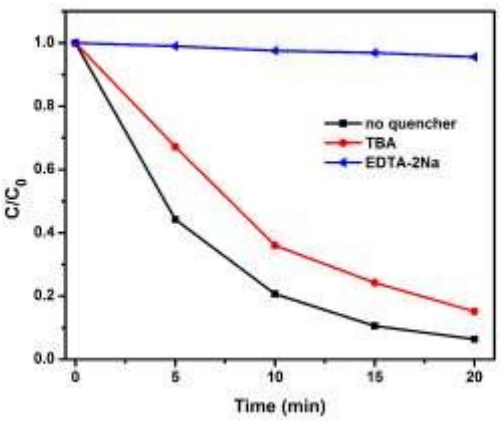

Fig. 10 Comparison of photocatalytic activities of 2mL-CDs/BiOBr nanocomposites for the degradation of RhB with or without adding EDTA-2Na and TBA.

Trapping experiments of hydroxyl radicals and holes were carried

out to explore the major active species in the photodegradation process with the 2mL-CDs/BiOBr nanocomposites. TBA and EDTA-Na were used as hydroxyl radicals scavengers and holes scavengers, respectively. As shown in Fig. 10, the photodegradation efficiency of RhB decreased slightly with the addition of TBA, indicating that dissolved •OH radicals were not the dominant active species in this process. In contrast, the addition of EDTA-Na exhibited a significantly negative influence on the photocatalytic activity, which indicated that the photogenerated holes were likely the main active oxidative species in the photodegradation of RhB with the 2mL-CDs/BiOBr sample.

Based on the above experimental results, we can see that the CDs can significantly increase the catalytic and photoelectrical activities of BiOBr. A possible mechanism of the enhanced photodegradation of RhB over CDs/BiOBr is proposed in Fig. 11.We propose that CDs play three important roles in the CDs/BiOBr nanocomposites during the photocatalytic process. An appropriate amount of CDs can darken the composite and thus enhance the absorption of visible light. The improved efficiency of CDs/BiOBr in the photocatalysis of RhB should be first attributed to its extended solar absorption spectrum, which is a prerequisite for good photocatalytic activity.[34]Secondly,due to the coupling and interaction between the CDs and BiOBr, the photogenerated electron could be injected easily and rapidly into the CDs and then activates dissolved oxygen in water.[35]Thirdly, it has been demonstrated that carbon nanostructures have a large electron-storage capacity, thus, the photonexcited electrons can be shuttled freely between BiOBr microspheres and CDs. During the photocatalytic process, CDs act as both electron acceptors and donors, in which the redundant electrons on BiOBr can be transferred to the conducting network of CDs and the electrons can also be easily transferred to the surface of BiOBr. Therefore, the CDs restrained the electron–hole pairs recombination probability and lengthened the lifetime of the charge carriers, consequently improving the photocatalytic activity in the CDs/BiOBr nanocomposites photocatalysts system.[17]Then, the electrons generated from sunlight irradiation combined with O_2adsorbed on the surface of composites to produce the superoxide anion radical (O_2^-), and the holes on the valence band (VB) of BiOBr subsequently oxidized and degraded the RhB. [6, 16]

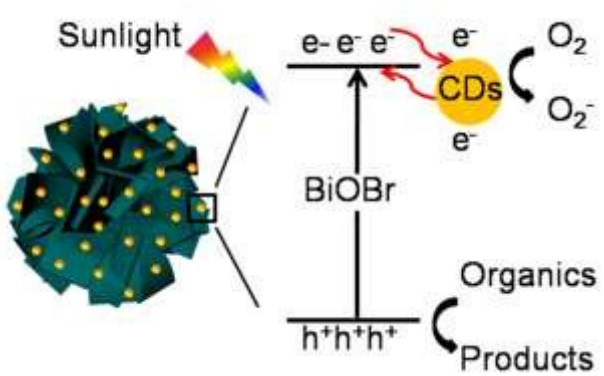

Fig. 11 Schematic illustration of the proposed mechanism for photodegradation process.

4. Conclusions

In conclusion, novel CDs/BiOBr nanocomposites with efficient photocatalytic activity under both UV and visible light irradiation have been successfully prepared for the first time. EDS and TEM analysis indicated CDs coupled the surface of sphere-like BiOBr uniformly. The CDs can extend the photoresponse range and improve the photogenerated electron–hole separation efficiency through storing and shuttling photogenerated electrons. CDs/BiOBr coupling system demonstrated significant improvement over bare BiOBr in the photodegradation of RhB with suitable loading amount of CDs, which exhibited high photocatalytic activity, excellent recyclability, and good efficiency. The trapping experiments of the radicals showed that the hole was the main reactive species during the photocatalysis process. Our work may encourage some new thoughts on the design of UV and visible light sensitive photocatalytic nanocomposites.

Acknowledgements

This work was supported by NSFC (Contract No. 51321091) and the Fundamental Research Funds of Shandong University.

Notes and references

State Key Laboratory of Crystal Materials, Shandong University, 27 Shandanan Road, Jinan 250100 (P.R. China). E-mail: xphao@sdu.edu.cn; wuyz@sdu.edu.cn

†Electronic Supplementary Information (ESI) available:

1 A. Fujishima and K. Honda, *Nature*, 1972, **238**, 37.
2 M. R. Hoffmann, S. T. Martin, W. Y. Choi and D. W.Bahnemann, *Chem. Rev.*,1995, **95**, 69.
3 J. G. Hou, Z. Wang, S. Q. Jiao and H. M. Zhu, *CrystEngComm*, 2012, **14**, 5923.
4 L. Kong, Z. Jiang, T. C. Xiao, L. F. Lu, M. O. Jones and P. P. Edwards, *Chem. Commun.*, 2011,**47**, 5512.
5 L. Kong, Z. Jiang, H. H. Lai, R. J. Nicholls, T. C. Xiao, M. O. Jones and P. P. Edwards, *J. Catal.*,2012, **293**,116.
6 J. Fu, Y. L. Tian, B. B. Chang, F. N. Xi and X. P. Dong, *J. Mater. Chem.*, 2012, **22**, 21159.
7 X. M. Tu, S. L. Luo, G. X. Chen and J. H. Li, *Chem. Eur. J.*, 2012, **18**, 14359.
8 S. Y. Chai, Y. J. Kim, M. H. Jung, A. K. Chakraborty, D. Jung and W. I. Lee, *J. Catal.*, 2009, **262**, 144.
9 Y. Zang and R. Farnood, *Appl. Catal. B: Environ.*, 2010, **79**, 334.
10 Z. P. Zhang, J. Zhang, N. Chen and L. T. Qu, Energy Environ. Sci., 2012, 5, 8869.
11 M. C. Beard, A. G. Midgett, M. C. Hanna, J. M. Luther, B. K. Hughes and A. J. Nozik, *Nano Lett.*,2010, **10**, 3019.
12 Y. P. Sun, B. Zhou, Y. Lin, W. Wang, K. A. S. Fernando, P. Pathak , M. J. Meziani, B. A. Harruff, X. Wang, H. F. Wang, P. G. Luo,H.Yang, M. E. Kose, B. Chen, L. M. Veca and S. Y. Xie, *J. Am. Chem. Soc.*, 2006, **128**, 7756.
13 A. B. Bourlinos, A. Stassinopoulos, D. Anglos, R. Zboril, M. Karakassides and E. P. Giannelis, *Small*, 2008,**4**, 455.
14 L. W. Zhang, H. B. Fu and Y. F. Zhu, *Adv. Funct. Mater.*, 2008, **18**, 2180.
15 H. T. Li, X. D. He, Z. H. Kang, H. Huang, Y. Liu, J. L. Liu, S. Y. Lian, C.A. Tsang, X. B. Yang and S. T. Lee, *Angew. Chem.*, 2010,**122**, 4532.
16 H. C. Zhang, H. Ming, S. Y. Lian, H. Huang, H. T. Li, L. L. Zhang, Y. Liu, Z. H. Kang and S. T. Lee, *Dalton Trans.*, 2011, **40**, 10822.
17 H. C. Zhang, H. Huang , H. Ming , H. T. Li , L. L. Zhang , Y. Liu and Z. H. Kang, *J. Mater. Chem.*, 2012, **22**, 10501.

18 H. T. Li, R. H. Liu, Y. Liu, H. Huang, H. Yu, H. Ming, S. Y. Lian and S. T. Lee, *J. Mater. Chem.*, 2012, **22**, 17470.

19 H. Yu, H. C. Zhang, H. Huang, Y. Liu, H. T. Li, H. Ming and Z. H. Kang, *New J. Chem.*, 2012, **36**, 1031.

20 B. Y. Yu and S. Y. Kwak, *J. Mater. Chem.*, 2012, **22**, 8345.

21 J. X. Xia, S. Yin, H. M. Li, H. Xu, L. Xu and Y. G. Xu, *Dalton Trans.*, 2011, **40**, 5249.

22 H. T. Li, X. D. He, Y. Liu, H. Huang, S. Y. Lian, S. T. Lee and Z. H. Kang, *Carbon*,2011, **49**, 605.

23 D. Tang, H. C. Zhang, H. Huang, R. H. Liu, Y. Z. Han, Y. Liu, C. Y. Tong and Z. H. Kang, *Dalton Trans.*, 2013, **42**, 6285.

24 P. Wang, B. B. Huang, X. Y. Qin, X. Y. Zhang, Y. Dai and M. H. Whangbo, *Inorg. Chem.*, 2009, **48**, 10697.

25 X. J. Yu, J. J. Liu,Y. C. Yu, S. L. Zuo and B. S. Li, *Carbon*, 2014, **68**, 718.

26 Y. H. Zhang, Z. R. Tang, X. Z. FuandY. J. Xu, *ACS Nano*, 2010,**4**, 7303.

27 J. Q. Pan, Y. Z. Sheng, J. X. Zhang, J. M. Wei, P. Huang, X. Zhang and B. X. Feng, *J. Mater. Chem. A*, 2014, **2**, 18082.

28 H. Xu, J. Yan, Y. G. Xu, Y. H. Song, H. M. Li , J. X. Xia,C. J. Huang and H. L. Wan, *Appl. Catal. B*, 2013,**129**, 182.

29 H. Ye, H. S. Park and A. J. Bard, *J. Phys. Chem. C*, 2011, **115**, 12464.

30 H. T. Li, Z. H. Kang, Y. Liu and S. T. Lee, *J. Mater. Chem.*, 2012, **22**, 24230.

31 H. J. Yu, Y. F. Zhao, C. Zhou, L. Shang, Y. Peng, Y. H. Cao, L. Z. Wu, C. H. Tung and T. R. Zhang, *J. Mater. Chem. A*, 2014, **2**, 3344.

32 Y. H. Ao, P. F. Wang, C. Wang, J. Hou and J. Qian, *Appl.Surf.Sci.*,2013, **271**, 265.

33 H. B. Fu, T. G. Xu, S. B. Zhu and Y. F. Zhu, *Environ. Sci. Technol.*, 2008, **42**, 8064.

34 W. Morales, M. Cason, O. Aina, N. R. Tacconi and K. Rajeshwar, *J. Am .Chem. Soc.*,2008, **130**, 6318.

35 F. Y. Zheng, Z. H. Wang, J. Chen and S. X. Li, *RSC Adv.*, 2014, **4**, 30605.

Table of contents

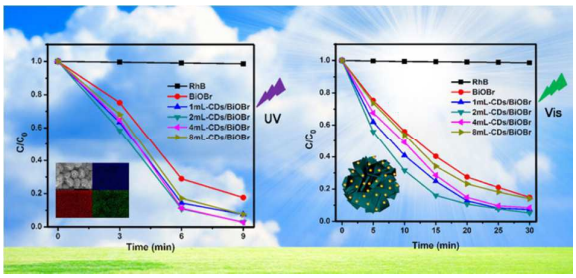

Novel CDs/BiOBr nanocomposites were prepared and both UV and visible light photocatalytic activities were enhanced.